Journal of Geophysical Research Oceans

Supporting Information for

Eddies in the Hawaiian Archipelago Region: formation, characterization, and potential implications on larval retention of reef fish

David Lindo-Atichati[1,2], Yanli Jia[3], Johanna L. K. Wren[4], Andreas Antoniades[2], and Donald R. Kobayashi[5]

[1]Department of Applied Ocean Physics and Engineering, Woods Hole Oceanographic Institution, Woods Hole, Massachusetts, USA
[2]Department of Earth and Planetary Sciences, American Museum of Natural History, New York, New York, USA
[3]International Pacific Research Center, University of Hawai'i at M̄anoa, Honolulu, Hawai'i, USA
[4]Joint Institute for Marine and Atmospheric Research, University of Hawai'i at M̄anoa, Honolulu, Hawai'i, USA
[5]Ecosystem Sciences Division, Pacific Islands Fisheries Science Center, National Oceanographic and Atmospheric Administration, Honolulu, Hawai'i, US

Contents of this file

Introduction

Included in the supporting information are additional simulations of larval dispersion in linear versus nonlinear eddies, additional simulations of larval dispersion in cyclonic linear versus anticyclonic linear eddies windward of the Hawaiian Archipelago, and additional simulations of larval dispersion in cyclonic linear versus anticyclonic linear eddies leeward of the Hawaiian Archipelago. Given the large distances between the eddies compared in the supplementary figures and the short distances traveled by eddies, figures side by side do not have the same lat/lon limits.

Text S1.
Additional simulations of larval dispersion in linear and nonlinear eddies are provided here. A linear mesoscale cyclonic eddy originated 245 km south of the Disappearing Island on August 27, 2012 (Figure S1a, blue dot). The average amplitude, radius, intensity, lifetime, and nonlinearity of that eddy were 2 cm, 61 km, 0.03 cm/km, 55 days, and 0.01. A total of 1000 synthetic larval fish were released at the centroid of the eddy and tracked during a 45-day period. Synthetic larvae dispersed northwest and covered a linear distance of 286 km from the release site to the average end location of all larvae (Figure S1a, blue cross). That eddy was embedded within the

HLC/NHRC system. Larval-fish were dispersed a mean distance (mean ± SD) of 171 ± 36 km away from the nearest reef habitat, the cloud of particles was concentrated along a filament line perpendicular to the island chain, and 95 % of larval fish spread a maximum distance of 113 km at the end of the 45-day dispersal period. Conversely, a nonlinear mesoscale anticyclonic eddy originated 600 km northeast of O`ahu on July 29, 2009 (Figure S1b, red dot). The average amplitude, radius, intensity, lifetime, and nonlinearity of that eddy were 0.7 cm, 33 km, 0.02 cm/km, 20 days, and 1.73. A total of 1000 synthetic larval fish were released at the centroid of the eddy and tracked during a 22-day period. Synthetic larvae remained tightly clustered by the nonlinear eddy and relatively stationary, covering only a linear distance of 46 km from the release site to the average end location of all larvae (Figure S1b, red cross). That eddy was located away from any main current system, north of the NHRC. Larval-fish were dispersed a mean distance (mean ± SD) of 533 ± 7 km away from the nearest reef habitat and 95 % of larval fish spread a maximum distance of 32 km at the end of the 45-day dispersal period. Again, a nonlinear eddy kept larval fish entrained and concentrated to a greater extent than a linear eddies.

Text S2.

Simulations of larval dispersion in linear eddies, cyclonic and anticyclonic, windward of the Hawaiian Archipelago are provided here. A linear mesoscale cyclonic eddy originated 100 km north of the Manualoa on August 10, 2012 (Figure S2a, blue dot). The average amplitude, radius, intensity, lifetime, and nonlinearity of that eddy were 3 cm, 52 km, 0.06 cm/km, 82 days, and 0.03. A total of 1000 synthetic larval fish were released at the centroid of the eddy and tracked during a 45-day period. Synthetic larvae dispersed west in a corkscrew pattern and covered a linear distance of 260 km from the release site to the average end location of all larvae (Figure S2a, blue cross). That eddy was embedded within the NHRC system. Larval-fish were were dispersed a mean distance (mean ± SD) of 68 ± 36 km away from the nearest reef habitat, the cloud of particles were distributed along the edge of the eddy to the north of Kaua`i, and 95 % of larval fish spread a maximum distance of 113 km at the end of the 45-day dispersal period. Conversely, a linear mesoscale anticyclonic eddy originated 115 km north of the Manualoa on May 19, 2012 (Figure S2b, red dot). That eddy was also embedded within the NHRC system. The average amplitude, radius, intensity, lifetime, and nonlinearity of that eddy were 1.3 cm, 23 km, 0.06 cm/km, 63 days, and 0.03. A total of 1000 synthetic larval fish were released at the centroid of the eddy and tracked during a 45-day period. Synthetic larvae remained entrained for the first half of the dispersal period, then dispersing them in two groups; one remaining on the windward side of the islands just north of Kaua`i and the other on the leeward side of the islands to the southwest of Kaua`i, covering a linear distance of 278 km from the release site to the average end location of all larvae (Figure S2b, red cross). They were dispersed a mean distance (mean ± SD) of 108 ± 46 km away from the nearest reef habitat and 95 % of larval fish spread a maximum distance of 374 km at the end of the 45-day dispersal period. The interaction of the anticyclonic eddy with the topography increased the spreading of larval fish.

Text S3.

Simulations of larval dispersion in linear eddies, cyclonic and anticyclonic, leeward of the Hawaiian Archipelago are provided here. A linear mesoscale cyclonic eddy originated 38 km northwest of the Big Island and 30 km south of Maui on August 16, 2009 (Figure S3a, blue dot). The average amplitude, radius, intensity, lifetime, and nonlinearity of that eddy were 5 cm, 53 km, 0.1 cm/km, 60 days, and 0.05. A total of 1000 synthetic larval fish were released at the centroid of the eddy and tracked during a 45-day period. Synthetic larvae dispersed south in a corkscrew pattern towards the NEC and covered a linear distance of 287 km from the release site to the average end location of all larvae (Figure S3a, blue cross). That eddy was located away from any main current system, in between the HLC, HLCC, and NEC systems. Larval-fish were dispersed a mean distance (mean ± SD) of 181 ± 42 km away from the nearest reef habitat and 95

% of larval fish spread a maximum distance of 268 km at the end of the 45-day dispersal period. Conversely, a linear mesoscale anticyclonic eddy originated 288 km southwest of Disappearing Island on June 29, 2009 (Figure S3b, red dot). That eddy was embedded within the NHLC system. The average amplitude, radius, intensity, lifetime, and nonlinearity of that eddy were 0.3 cm, 25 km, 0.01 cm/km, 54 days, and 0.01. A total of 1000 synthetic larval fish were released at the centroid of the eddy and tracked during a 45-day period. Synthetic larvae stretched to the south then west covering a linear distance of 235 km from the release site to the average end location of all larvae (Figure S3b, red cross). They were dispersed a mean distance (mean ± SD) of 285 ± 17 km away from the nearest reef habitat and 95 % of larval fish spread a maximum distance of 187 km at the end of the 45-day dispersal period. The low value of nonlinearity of the anticyclonic eddy, which was the lowest value of the set the eddies shown in Figure 8 and Figures S1-S3, favored the stretching of larval fish. Most larval fish were left behind in that very linear eddy.

Text S4-S5

A seasonal variability, defined as a higher rate of eddy births in spring than in fall, was clear in the whole analysis region for eddies with any radius (Figures S4a and S5a). In the Leeward and Windward region, however, that seasonal variability was less apparent for eddies with radius less than 25 km (Figures S4b) and there was not seasonal variability for eddies with radius greater than 25 km (Figures S5b).

Text S6-S7

Rossby number, defined here as the ratio of relative vorticity to planetary vorticity, is computed from both the model's surface velocity and the model's surface geostrophic velocity. Figures S4 and S5 show the potential errors associated with assuming geostrophic balance in the vicinity of the Big Island of Hawaii. Anticyclonic eddy rotation tends to be underestimated by the geostrophic flow (for example, the linear anticyclonic eddy within which larval fish were seeded, Figure S6) and cyclonic eddy rotation tends to be overestimated by the geostrophic flow (for example, the nonlinear cyclonic eddy within which larval fish were seeded, Figure S7).

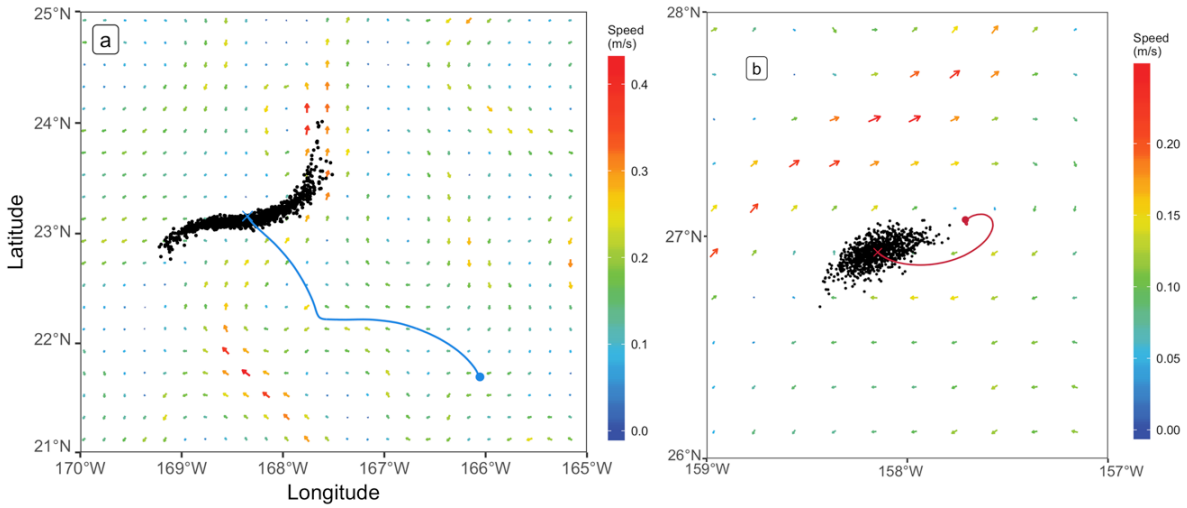

Figure S1. Distribution of synthetic coral reef larval fish at the end of their pelagic larval duration when they are released in eddies with different nonlinearities. (a) Start location of 1000 larval fish at the center of a linear cyclonic eddy on August 27, 2012 (blue dot), average trajectory of all larval fish during their pelagic larval duration (blue curve), individual end locations (black dots), and average end location (blue cross) of all larval fish on October 12, 2012. (b) Start location of 1000 larval fish at the center of a nonlinear anticyclonic eddy on July 29, 2009 (red dot), average trajectory of all larval fish during a pelagic larval duration of 22 days (red curve), and individual end locations (black dots) and average end location (red cross) of larval fish on August 20, 2009. Surface geostrophic currents from MITgcm are superimposed for the end day of each simulation. The lifetime of both eddies is longer than the duration of the simulations.

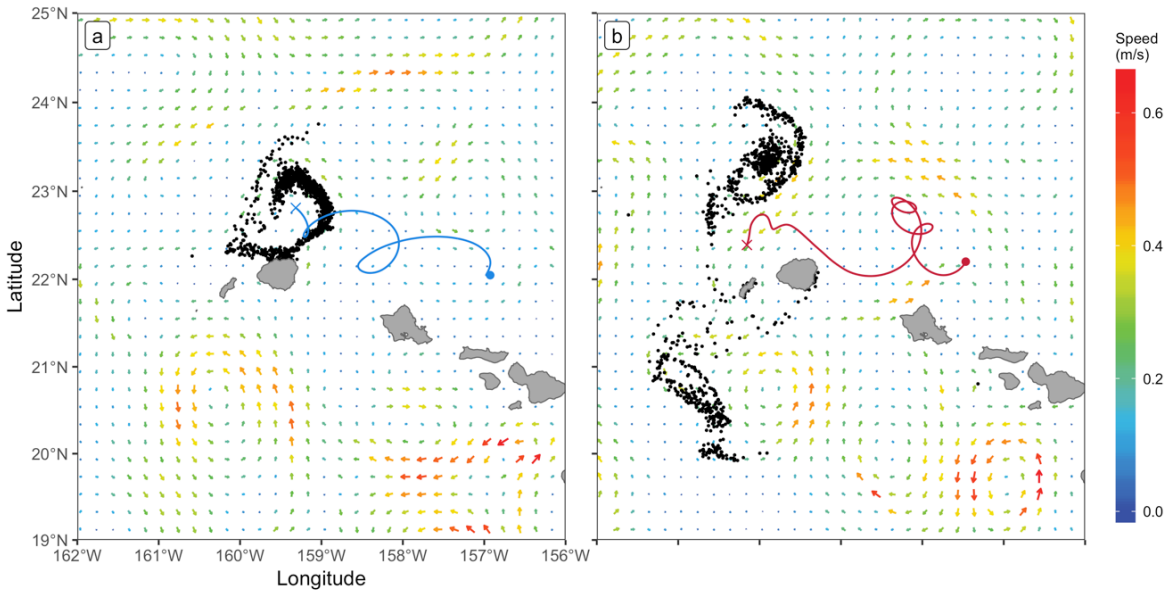

Figure S2. Distribution of synthetic coral reef larval fish at the end of their pelagic larval duration when they are released in eddies with different polarity eastward of the Hawaiian Archipelago. (a) Start location of 1000 larval fish at the center of a linear cyclonic eddy on August 10, 2012 (blue dot), average trajectory of all larval fish during their pelagic larval duration (blue curve), individual end locations (black dots), and average end location (blue cross) of all larval fish on September 25, 2012. (b) Start location of 1000 larval fish at the center of a linear anticyclonic eddy on May 19, 2012 (red dot), average trajectory of all larval fish during a pelagic larval duration of 45 days (red curve), and individual end locations (black dots) and average end location (red cross) of larval fish on July 4, 2012. Surface geostrophic currents from MITgcm are superimposed for the end day of each simulation. The lifetime of both eddies is longer than the duration of the simulations.

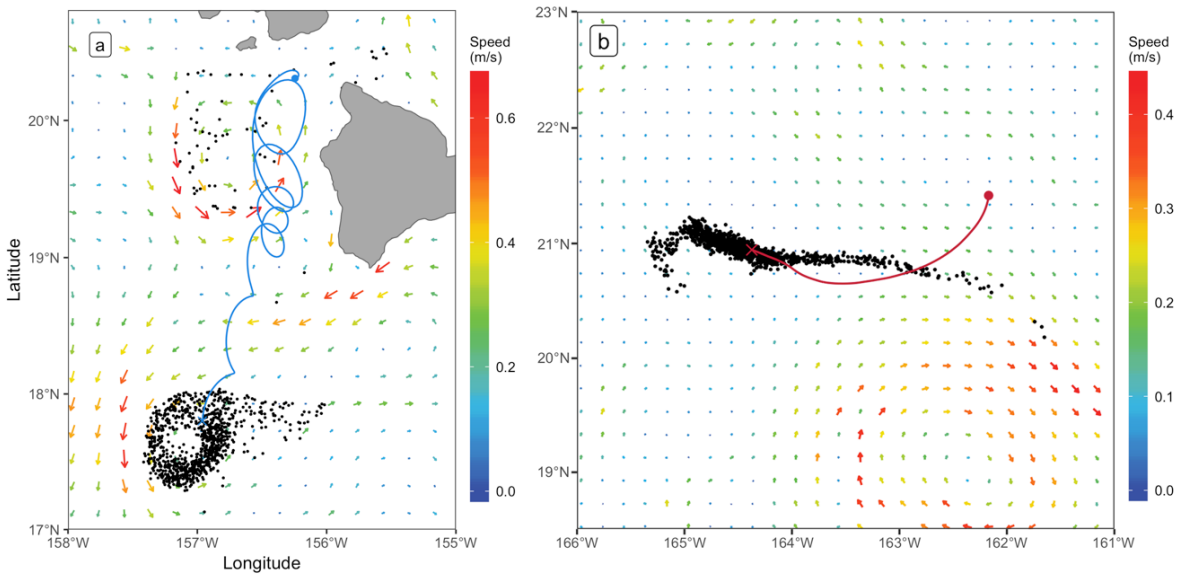

Figure S3. Distribution of synthetic coral reef larval fish at the end of their pelagic larval duration when they are released in eddies with different polarity westward of the Hawaiian Archipelago. (a) Start location of 1000 larval fish at the center of a linear cyclonic eddy on August 16, 2009 (blue dot), average trajectory of all larval fish during their pelagic larval duration (blue curve), individual end locations (black dots), and average end location (blue cross) of all larval fish on October 1, 2009. (b) Start location of 1000 larval fish at the center of a linear anticyclonic eddy on June 29, 2009 (red dot), average trajectory of all larval fish during a pelagic larval duration of 45 days (red curve), and individual end locations (black dots) and average end location (red cross) of larval fish on September 12, 2009. Surface geostrophic currents from MITgcm are superimposed for the end day of each simulation. The lifetime of both eddies is longer than the duration of the simulations.

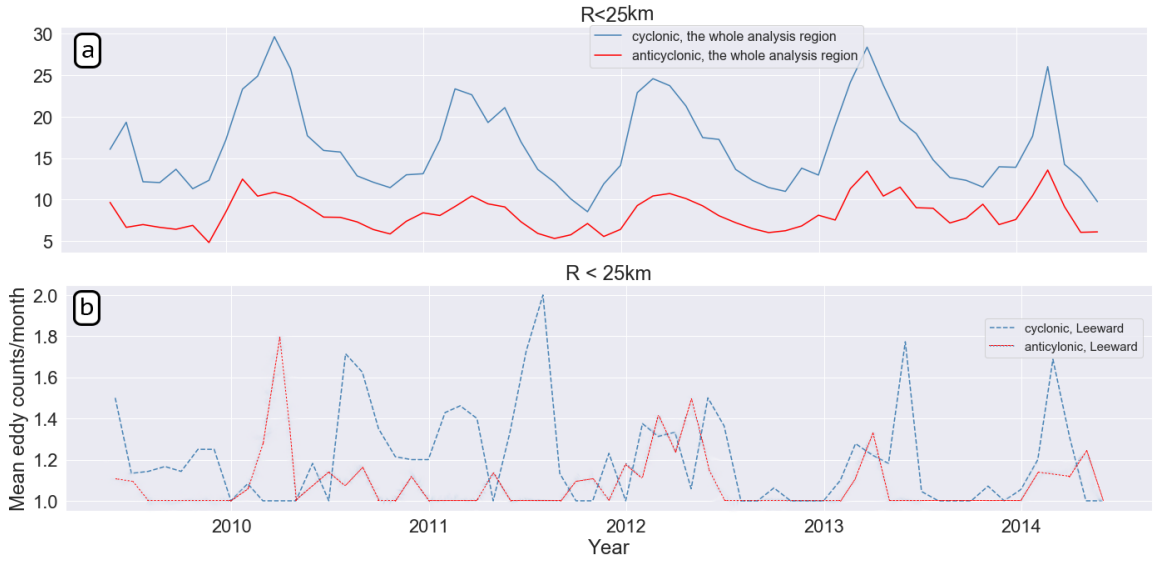

Figure S4. Monthly counts of cyclonic and anticyclonic eddies with radius less than 25 km for the whole of the analysis region, and (b) for the Leeward and Windward regions over the 5-year study period.

Figure S5. (a) Monthly counts of cyclonic and anticyclonic eddies with radius equal or greater than 25 km for the whole of the analysis region, and (b) for the Leeward and Windward regions over the 5-year study period.

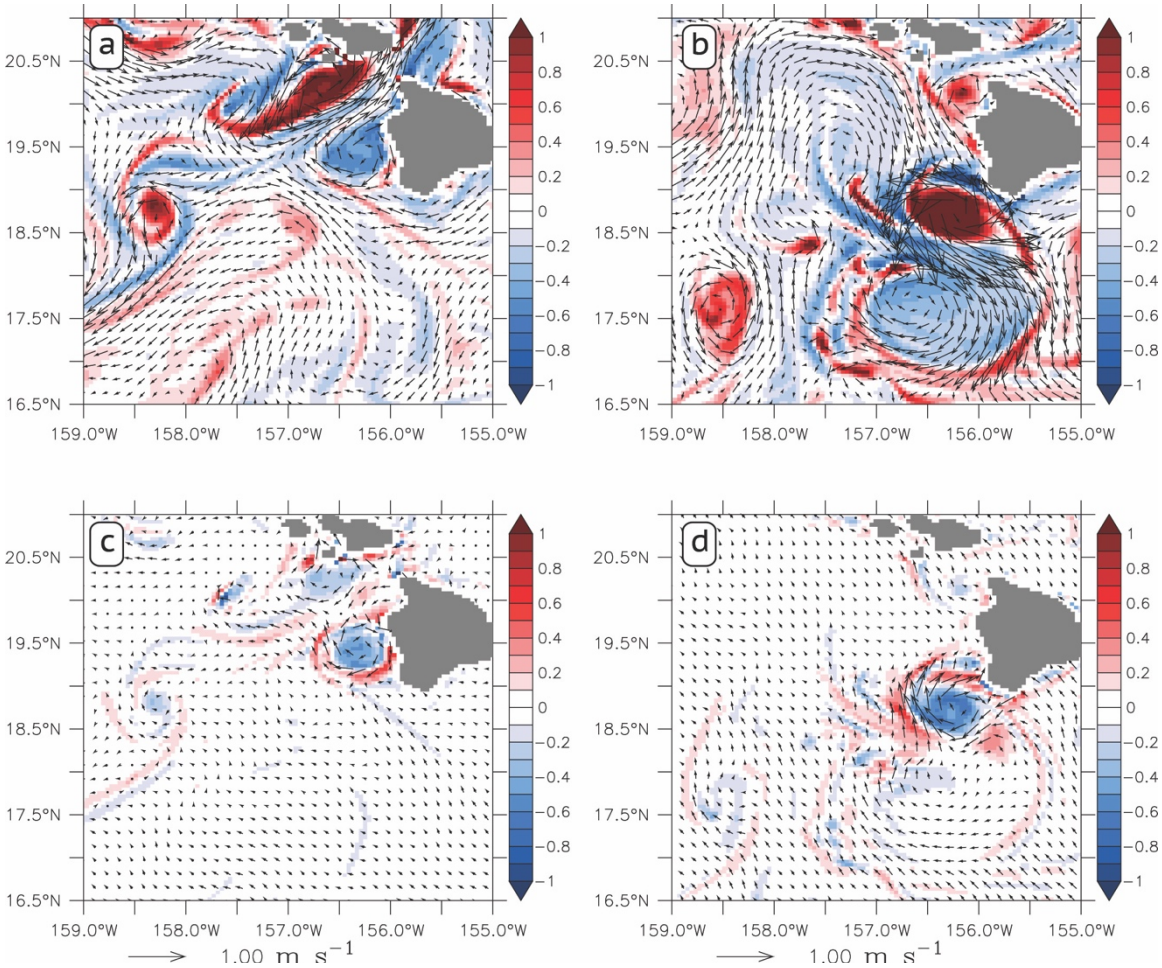

Figure S6. Rossby number (color) computed from the model's surface geostrophic velocity (upper panels), overlaid with the surface geostrophic velocity (vector), and the difference in Rossby number between that computed from the model's surface velocity and that from the model's surface geostrophic velocity (lower panels), overlaid with the corresponding velocity difference: (a) and (c) for November 25, 2011, corresponding to the start time of Figure 8a (linear anticyclonic eddy); and (b) and (d) for April 20, 2010, corresponding to the start time of Figure 8b (nonlinear cyclonic eddy). For the linear anticyclonic eddy, the Rossby number computed from geostrophic velocity is -0.57 and the difference is -0.44 in the early stage of its life (Figure S6a and c). For the nonlinear cyclonic eddy, the Rossby number computed from geostrophic velocity is 1.03 and the difference is -0.28 in the early stage of its life (Figure S6b and d).

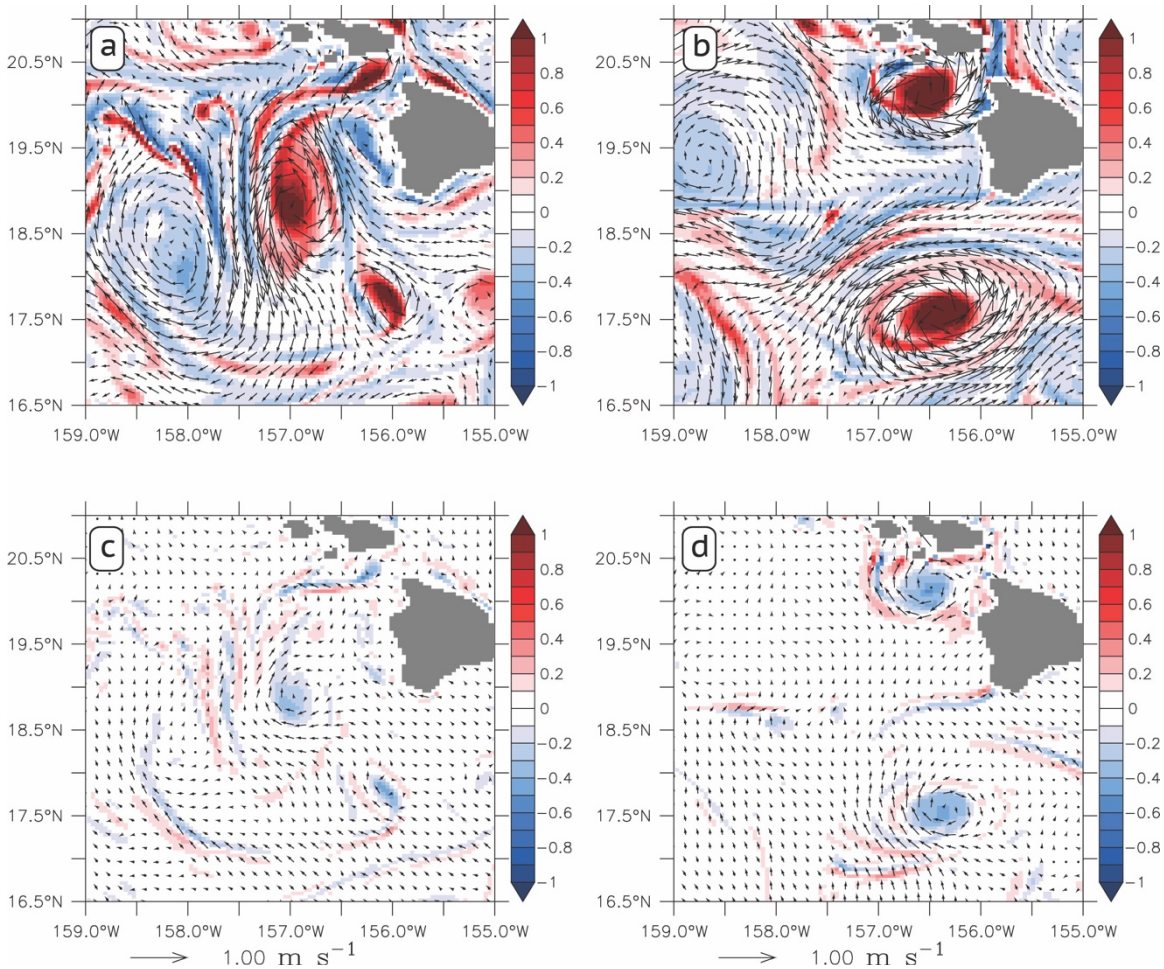

Figure S7. As for Figure S6 except (a) and (c) for January 8, 2012, corresponding to the end time of Figure 8a (linear anticyclonic eddy); and (b) and (d) for June 3, 2010, corresponding to the end time of Figure 8b (nonlinear cyclonic eddy). For the linear anticyclonic eddy, the Rossby number computed from geostrophic velocity is -0.44 and the difference is -0.07 at day 45 of its lifetime (Figure S7a and c). For the nonlinear cyclonic eddy, the Rossby number computed from geostrophic velocity is 1.48 and the difference is -0.50 at day 45 of its lifetime (Figure S7b and d).